LAWRENCE
LIVERMORE
NATIONAL
LABORATORY

UCRL-JRNL-207259

Activation Energy for Grain Growth in Aluminum Coatings

A. F. Jankowski, J. L. Ferreira, J. P. Hayes

October 15, 2004

Thin Solid Films

Activation Energy for Grain Growth in Aluminum Coatings

Alan Jankowski[1], James Ferreira[1], and Jeffrey Hayes[2]

Lawrence Livermore National Laboratory

[1]Chemistry & Materials Science, and [2]Mechanical Engineering

Livermore, CA 94551-9900, U.S.A.

ABSTRACT

To produce a specific grain size in metallic coatings requires precise control of the time at temperature during the deposition process. Aluminum coatings are deposited using electron-beam evaporation onto heated substrate surfaces. The grain size of the coating is determined upon examination of the microstructure in plan view and cross-section. Ideal grain growth is observed over the entire experimental range of temperature examined from 413 to 843 K. A transition in the activation energy for grain growth from 0.7 to 3.8 eV•atom^{-1} is observed as the temperature increases from <526 K to >588 K. The transition is indicative of the dominant mechanism for grain growth shifting with increasing temperature from grain boundary to lattice diffusion.

INTRODUCTION

The synthesis of fully dense coatings to several hundred microns in thickness in the form of free standing foils and as coated substrates is of growing interest for material behavior studies under dynamic loading conditions.[1-3] To pursue the controlled growth of specimens with grain sizes that range from 0.1 μm to 1 cm presents a challenge for preparation by physical vapor deposition technology. The use of electron-beam evaporation is an established and appropriate process to systematically deposit such thick coatings as deposition high rates in excess of 0.1 $\mu m \cdot s^{-1}$ can be routinely achieved.[4] The classic zone model(s) for growth of vapor deposits provide an excellent starting point for selecting the process conditions required to produce dense metal coatings.[5-11] For the case of evaporative deposits, it's primarily the surface and bulk diffusion processes that progressively affect grain size growth with increasing temperature from dense columnar-type microstructures to equiaxed polycrystalline solids.[11] Within this context, we investigate the electron-beam evaporation conditions relevant to the formation of aluminum polycrystalline deposits.

The time at temperature affects the coating grain size. In order to quantify the kinetics of grain growth, the coating temperature during the deposition process should be nearly isothermal. Typical investigations of high-rate evaporation processes have a focus on a narrow range of substrate temperatures relative to the melt point but do not document the time at temperature.[6-7] The qualitative variation in microstructure and grain size observed for aluminum coatings [12], evaporated over a wide range (383 to 793 K) of substrate temperatures confirm the basic morphologies of the zone model. Although a quantitative analysis of the growth kinetics at temperature above 537 K was recently reported [13], a detailed study of growth kinetics at lower temperatures remains incomplete. New experimental results are presented for the time evolution of grain size from the micron-to-millimeter scale for the electron-beam deposition of aluminum

coatings up to 100 μm in thickness. The kinetics is evaluated with respect to the grain growth law. Analysis of the activation energy and the mechanism for grain growth are made for both temperature ranges above and below half the melt point (T_m).

EXPERIMENTAL METHODS

The electron-beam evaporation method is used to produce a large range of grain size (d_g). The vacuum chamber is cryogenically pumped to a base pressure less than 1.3×10^{-5} Pa. A 0.9999 pure aluminum target is melted in a 40 cm^3 pocket-crucible using an electron-beam operated at 10 kV with a discharge current range of 200-600 mA. The source-to-substrate distance range of 10-15 cm facilitates higher deposition rates for the synthesis of thick coatings. A tantalum substrate platen is resistively heated using a boron-nitride heating element. The 3 mm sq substrates used are 50-75 μm thick mica sheets and 125-500 μm thick lithium fluoride (LiF) crystals. The substrates are fastened to the platen using a hard mask. The deposition rate is monitored using a calibrated 6 MHz gold-coated oscillating quartz crystal. The final coating thickness is measured using a contact profilometer

The baseline temperature of the substrate platen is feedback-control regulated. However, it's the actual temperature of the coating (T_c) that needs to be measured for determination of the grain growth kinetics. In these experiments, thermocouples are placed in firm contact with substrate surface as well as platen. As the deposition process proceeds, the substrate surface thermocouples are embedded into the coating. This measurement provides the actual coating temperature during the deposition process. Although in equilibrium and numerically equivalent prior to the deposition process, the coating temperature may not equal the substrate temperature (T_s) during deposition. Independent measurements of the coating and substrate have revealed a significant temperature gradient that results during the electron-beam deposition process.[13]

This method of temperature measurement is especially important, for example, when the substrate is a thermal insulator as well as for the high-rate deposition of aluminum.[13-14] A coating temperature range of 413-843 K is used in this study, noting a T_m for aluminum of 933 K, in order to ensure fully dense coatings.[5, 9-12]

The microstructure of the aluminum coating surface is imaged in plan view using a scanning electron microscope (SEM). The method of x-ray diffraction (XRD) provides a measure of the crystalline orientation of the grains in the aluminum coatings. The coating surfaces are scanned in the θ/2θ mode using Cu *K*a radiation. The grain size is quantified from the plan view images using the lineal intercept method.[15] A circular test figure of known perimeter (P) is randomly applied to the image of the coating surface at magnification (M). The number (N) of test-circle intersections are counted with grain boundaries. The average grain diameter (d_g) for cubic grains equals 2.25·L where the average lineal intercept (L) equals $n \cdot P\ (M \cdot N)^{-1}$ for a total number (n) of applications. That is, the average grain diameter is

$$d_g = 2.25 \cdot \{n \cdot P\ (M \cdot N)^{-1}\}. \qquad (1)$$

The value for d_g determined in this way from eqn. (1) is equivalent to the lineal intercept value determined from cross-section views of the average column width.[13]

RESULTS & ANALYSIS

The coating temperature is different than the substrate platen temperature during the electron beam deposition of the aluminum coating on thermally insulating substrates as mica and LiF.[13] For example, a temperature profile with time is shown in Fig. 1 for a 34 μm thick coating deposited at a rate of 30 $nm \cdot sec^{-1}$ onto a mica substrate. This Al deposition is initiated at time (t) equals zero and concludes at 19 min. In general, the coating temperature (T_c) increases

with the substrate temperature (T_s) as shown in Fig. 2. However, the (T_c) may vary at constant (T_s) as dependent on the heat radiated from the evaporation source under varying deposition rate conditions and at different source-to-substrate distances. The T_c values plotted in Fig. 2. are the time-averaged measurements during the deposition, i.e. when the substrate is exposed to the evaporation source. These values are referenced during the grain size analysis to follow.

The SEM images of the Al coatings reveal the basic features of the microstructure. The grain boundaries are well defined at the Al coating surface in the SEM plan view images which are then used for the measuring grain size. For example, a progressive increase in grain size with increasing temperature is seen in the images of Fig(s). 3a-3c. from 10.9±0.7 μm for a 334±8 °C deposit (Fig. 3a.) to 46.5±1.6 μm for a 415±17 °C deposit (Fig. 3b.), to a 3 mm sq single-crystal for a 540±15 °C deposit (Fig. 3c.) in which grain boundaries are not present.

The XRD scans of the Al coatings reveal an invariant (111) growth texture, as seen in (Fig. 4.) the representative θ/2θ scan for a 535 °C deposit. The only peaks observable are the (111) and (222) Bragg reflections at 38.33º and 82.25º (2θ), respectively. In comparison, heteroepitaxial conditions for the growth of either (111) or (110) aluminum can be achieved using (0001) sapphire substrates.[16]

An analysis of grain growth is made since the grain size of the Al coatings is measured as function of a nearly isothermal-coating temperature (T_c) during the deposition over a defined time interval (t). The grain growth law provides the relationship to compute the activation energy (Q) needed for grain growth during deposition of the aluminum coatings. The grain growth law relates grain size as proportionate to time raised to the power n.[17] That is,

$$d_g \alpha t^n \qquad (2)$$

where for ideal grain growth, n equals 0.5. To determine if ideal grain does indeed occur, the grain size squared (d_g^2) is plotted versus time (t) in Fig. 5. The grain size data is grouped into narrow temperature-range intervals in Fig. 5 for this purpose. In this plot, as well as the analysis to follow,

$$d_g^2 = [d_g(f)]^2 - [d_g(i)]^2 \quad (3)$$

where $d_g(i)$ is the initial grain size and $d_g(f)$ is the final grain size, noting that $d_g(i)$ equals zero for the electron-beam deposited coatings. For the higher temperature data, the d_g^2 values plotted are reduced by a multiplication factor (as listed in the Fig. 5 legend) to allow an analysis of all temperatures ranges on this one graph. Similarly, for the lower temperature data, the d_g^2 values plotted are magnified by a multiplication factor as listed in the Fig. 5. legend. A linear relationship is observed for the "d_g^2 vs. t" curves for all coating temperatures confirming ideal grain growth, i.e. n equals 0.5. Therefore, a plot of T_c^{-1} versus $\ln(d_g^2 \cdot t^{-1})$ (seen in Fig. 6) should yield a linear variation from which a value for the slope equals $\{-Q \cdot (2R)^{-1}\}$, where R is the molar gas constant (8.314 $J \cdot mol^{-1} \cdot K^{-1}$).[18]

A linear regression analysis is used to compute the activation energy (Q) corresponding with the slope for the linear regime(s) of the "$1000 \cdot T_c^{-1}$ vs. $\ln(d_g^2 \cdot t^{-1})$" data plotted in Fig. 6. That is, the activation energy is determined from the relationship,

$$Q = -(2R) \cdot \partial[\ln(d_g^2 \cdot t^{-1})] \cdot \partial[T_c^{-1}]^{-1} \quad (4)$$

A distinct transition is seen in Fig. 6 from a low temperature (<526 K) to high temperature (>588 K) regime. The low temperature data of this present study (in Fig. 6) is supplemented with a plot of the grain boundary self-diffusion data determined by Volin, et.al. [19]. The self-diffusion data was generated from a transmission electron microscopy study of void-shrinkage kinetics over the

323-453 K temperature range in 100 μm thick pure Al ribbons that contained quenched in vacancies.[19]

The temperature transition seen in the (Fig. 6) plot of "$1000 \cdot T_c^{-1}$ vs. $\ln(d_g^2 \cdot t^{-1})$" by two distinct linear regimes indicates a change in the dominant mechanism for grain growth from dislocation (grain boundary) to volume (lattice) diffusion as the coating temperature increases. We find an activation energy representative of volume diffusion (Q_{vol}) equal to 3.8 $eV \cdot atom^{-1}$ (368 $kJ \cdot mol^{-1}$) that is in close agreement with a preliminary study of the high temperature regime [13] for which an activation energy of 4.1 $eV \cdot atom^{-1}$ was reported. Similarly, a slightly lower activation energy of 2.9 $eV \cdot atom^{-1}$ (283 $kJ \cdot mol^{-1}$) is measured for Al^{27} tracer diffusion in aluminum [20] over the 723-923 K temperature range noting use of the $-Q \cdot (2R)^{-1}$ formalism and the conversion that 96 $kJ \cdot mol^{-1}$ equals 1 $eV \cdot atom^{-1}$. Likewise, a value of 2.8 $eV \cdot atom^{-1}$ (266 $kJ \cdot mol^{-1}$) is determined from the Van Liempt relation (of $Q = 0.0285\ T_m$ in units of $kJ \cdot mol^{-1}$) for normal self diffusion.[21] Also, for comparison, a value of 2.6 $eV \cdot atom^{-1}$ is reported for thermally activated diffusion in aluminum-copper alloy films over the 673-773 K temperature range.[22] For the low temperature regime, a lower value of 0.7 $eV \cdot atom^{-1}$ (67 $kJ \cdot mol^{-1}$) is measured as the activation energy representative of dislocation diffusion (Q_{disl}) which is in agreement with the value reported [19] in the grain boundary self-diffusion study.

The difference between the two activation energies (for the high and low temperature regimes) by a factor of two or more is in agreement with a compilation of findings by Martin and Perraillon.[23] They note for the case of self-diffusion, which applies Al grain growth, that the apparent activation energy in a grain boundary is roughly 0.4-0.6 time the activation energy for bulk diffusion. Consequently, as in the case of short-circuit diffusion [24] in Harrison's A regime [25], it may be inferred that the effective diffusion (D_{eff}) for grain growth can be considered attributable to the volume fraction (f) contribution of dislocations with respect to dislocation

diffusion (D_{disl}) and volume (lattice) diffusion (D_{vol}) noting that the diffusion coefficient is proportional to the exponential of $-Q\cdot(2R\cdot T)^{-1}$. That is, an arithmetic rule-of-mixtures summation as

$$D_{eff} = (1-f)\cdot D_{vol} + f\cdot D_{disl} \qquad (5)$$

In general, the similarity of the present case exists wherein diffusion occurs by more than one mechanism.[26-27]

CONCLUSIONS

A grain size dependence on the coating temperature with respect to the melt point (T_m) is found for the evaporative deposition of aluminum. Ideal grain-growth behavior is observed in coatings over the temperature range of $(0.4\text{-}0.9)\cdot T_m$. With measurement of the coating temperature and grain size, we've determined the activation energy for grain growth in aluminum coatings as 3.8 $eV\cdot atom^{-1}$ above $0.63\cdot T_m$, and as 0.7 $eV\cdot atom^{-1}$ below $0.56\cdot T_m$. The transition is indicative of the dominant mechanism for grain growth shifting with increasing temperature from dislocation (grain boundary) to volume (lattice) diffusion.

ACKNOWLEDGMENTS

The authors thank Prof. T.G. Nieh for his instructive comments and references. This work was performed under the auspices of the U.S. Department of Energy by University of California, Lawrence Livermore National Laboratory under contract No. W-7405-Eng-48.

REFERENCES

1. J. Edwards, K.T. Lorenz, B. Remington, S. Pollaine, J. Colvin, D. Braun, B. Lasinski, D. Reisman, J. McNaney, J. Greenough, R. Wallace, H. Louis, and D. Kalantar, Phys. Rev Lett. 92 (2004) 75002.

2. B. Yaakobi, D. Meyerhofer, T. Boehly, J. Rehr, B. Remington, P. Allen, S. Pollaine, and R. Albers, Phys. Rev. Lett. 92 (2004) 95504.

3. T. Ditmire, E. Grumbrell, R. Smith, L. Mountford, and M. Hutchinson, Phys. Rev. Lett. 77 (1996) 498.

4. R. Nimmagadda and R.F. Bunshah, J. Vac. Sci. Technol., 8 (1971) VM85.

5. R.F. Bunshah and R.S. Juntz, Metall. Trans. 4 (1973) 21.

6. M.A. Sherman, R.F. Bunshah, and H.A. Beale, J. Vac. Sci. Technol. 12 (1975) 697.

7. N. Agarwal, N. Kane, and R.F. Bunshah, J. Vac. Sci. Technol. 12 (1975) 619.

8. R.F. Bunshah, J. Vac. Sci. Technol. 11 (1974) 814.

9. B.A. Movchan, and A.V. Demchishin, Phys. Met. Metallogr., 28 (1969) 83.

10. R.F. Bunshah, J. Vac. Sci. Technol., 11 (1974) 633.

11. J.A. Thornton, J. Vac. Sci. Technol. A, 4 (1986) 3059.

12. M. Neirynck, W. Samaey, and L. Van Poucke, J. Vac. Sci. Technol. 11 (1974) 647.

13. A.F. Jankowski and J.P. Hayes, Thin Solid Films 447-448 (2004) 568.

14. A.N. Pargellis, J. Vac. Sci. Technol. A, 7 (1989) 27.

15. J.E. Hilliard, Metal Progr., 85 (1964) 99.

16. D. Medlin, K. McCarty, R. Hwang, S. Guthrie, and M. Baskes, Thin Solid Films 299 (1997) 110.

17. R.E. Reed-Hill, Physical Metallurgy Principles, Van Nostrand, New York, NY (1973) pp. 304-310.

18. P. Feltham and G.J. Copley, Acta Met. 6 (1958) 539.

19. T.E. Volin, K.H. Lie, and R.W. Balluffi, Acta Met. 19 (1971) 263.

20. T.S. Lundy and J.F. Murdock, J. Appl. Phys. 33 (1962) 1671.

21. J.A.M. Van Liempt, Z. Phys. 96 (1935) 534.

22. W.C. McBee and J.A. McComb, Thin Solid Films 30 (1975) 137.

23. G. Martin and B. Perraillon, in Grain Boundary Structure and Kinetics, ASM Materials Science Seminar, ASM, Metals Park, OH (1979) p. 239.

24. E.W. Hart, Acta Metall. 5 (1957) 597.

25. L.G. Harrison, Trans. Farad. Soc. 57 (1961) 1191.

26. J.L. Bocquet, G. Brébee, and Y. Limoge, in Physical Metallurgy, eds. R. W. Cahn and P. Haasen, 3rd Edition, North Holland Physics Publishing, Amsterdam (1983) pp. 403, 415.

27. A. Seeger and H. Mehrer, in Vacancies and Interstitials in Metals, eds. A. Seeger, D. Schumacher, and J. Diehl, North Holland, Amsterdam (1970) p. 1.

FIGURE CAPTIONS

Figure 1. This time-temperature plot displays the thermal history during an electron-beam deposition of aluminum as measured in the coating (T_c) and on the substrate platen (T_s).

Figure 2. The coating temperature (T_c) varies with the substrate temperature (T_s) during the electron-beam deposition of aluminum coatings at various deposition rates and at various source-to-substrate distances.

Figure 3. The scanning electron micrographs of aluminum coating surfaces for depositions at coating temperatures of (a) 334 °C, (b) 415 °C, and (c) 540 °C.

Figure 4. A plot of intensity versus 2θ position, in this x-ray diffraction scan of a 535 °C deposit, reveals the (111) texture of the aluminum coating.

Figure 5. The linear curves of grain size squared (d_g^2) versus time (t) confirm the assumption of ideal grain growth over the full temperature range measured for the aluminum coatings during electron-beam deposition.

Figure 6. Linear fits to the curves in the plot of $1000 \cdot T^{-1}$ versus $\ln(d_g^2 \cdot t^{-1})$ follows the assumption of ideal grain growth for these aluminum coatings at low temperatures where grain boundary diffusion is dominant, and at high temperature where lattice (volume) diffusion is dominant.

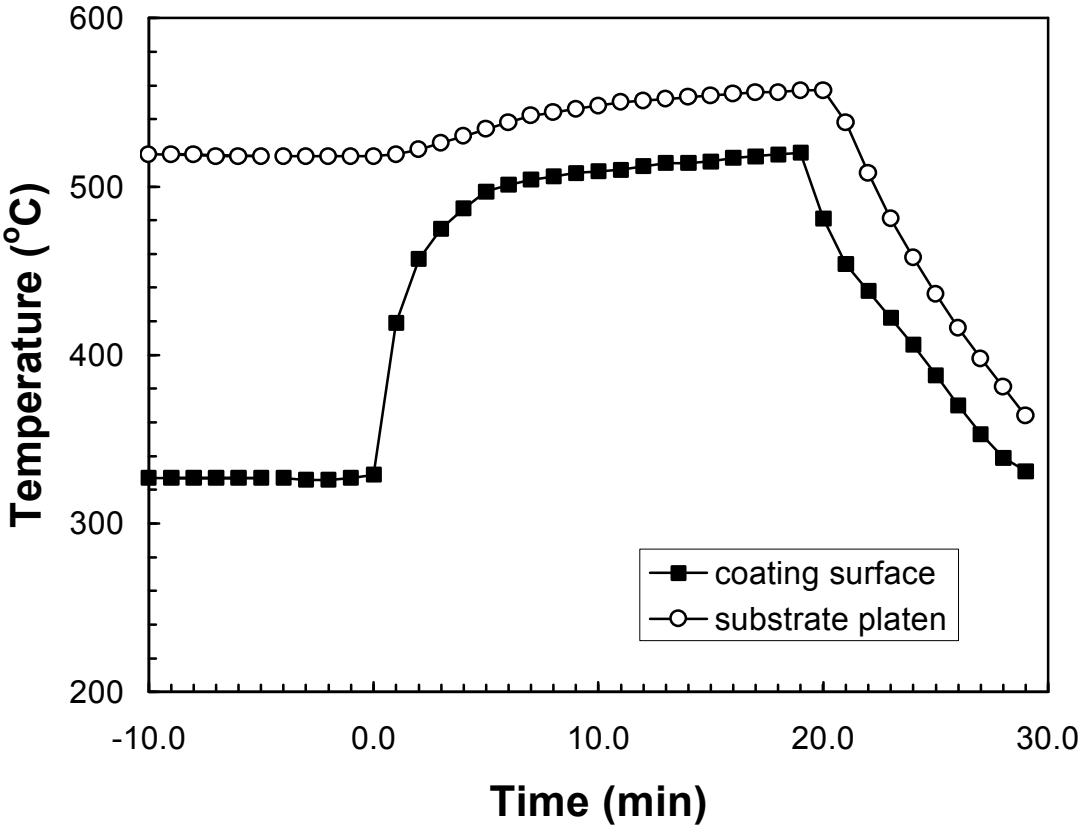
600
500
400
300
200
Temperature (°C)
-10.0
0.0
10.0
20.0
30.0
Time (min)
coating surface
substrate platen

Figure 1.

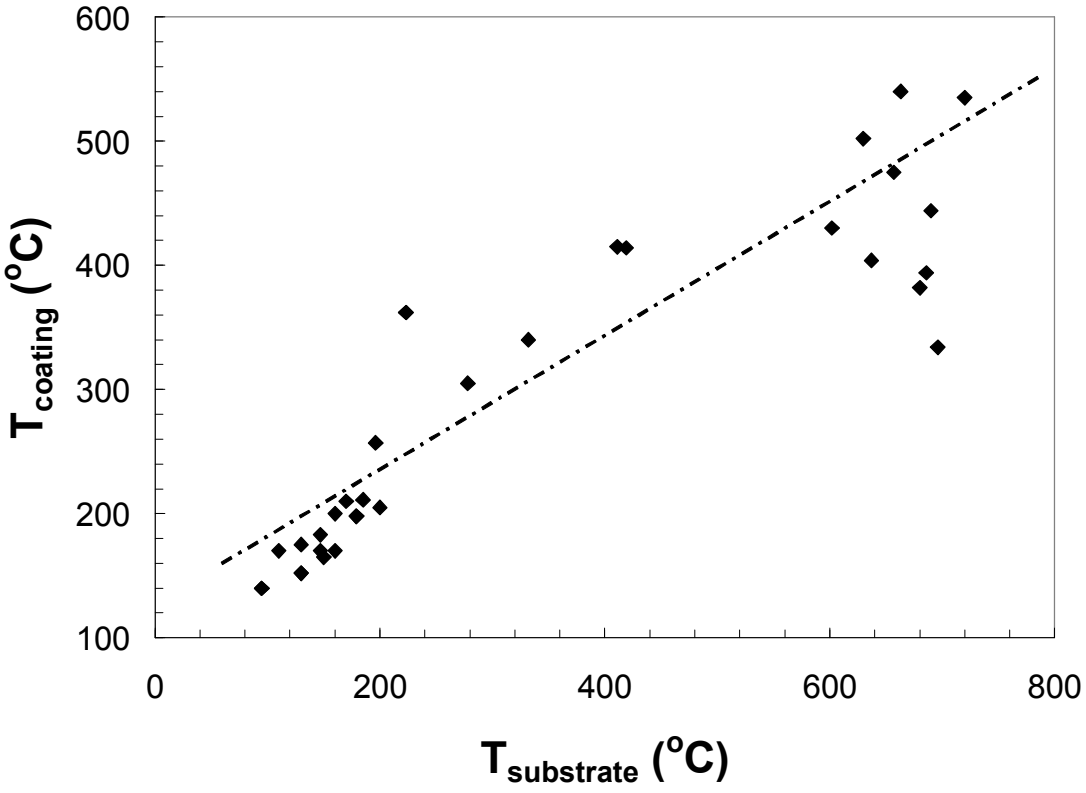
600
500
400
300
200
100
0
200
400
600
800
T coating (°C)
T substrate (°C)

Figure 2.

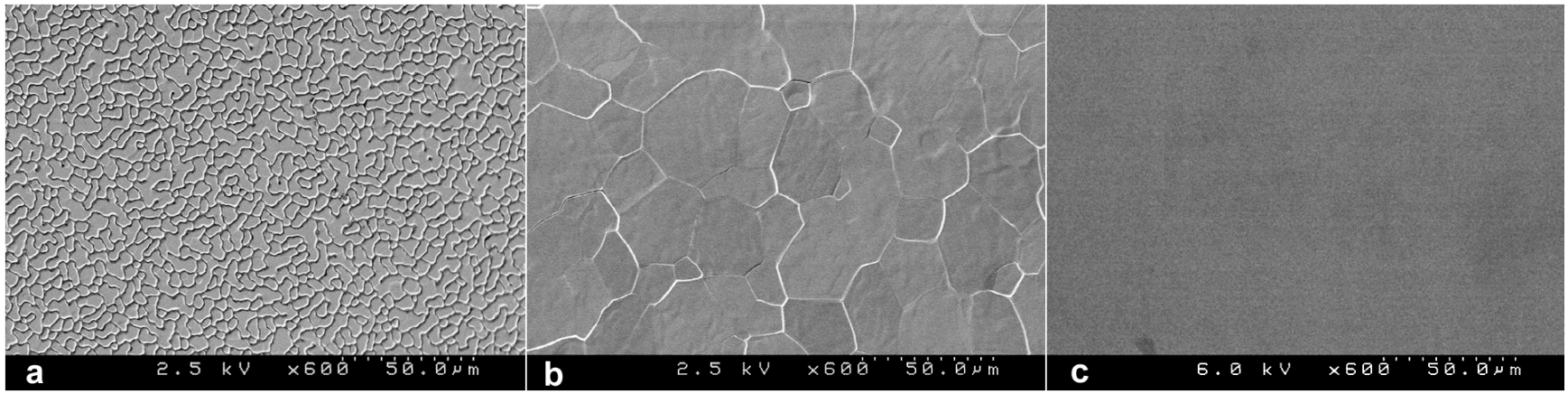

Figure 3.

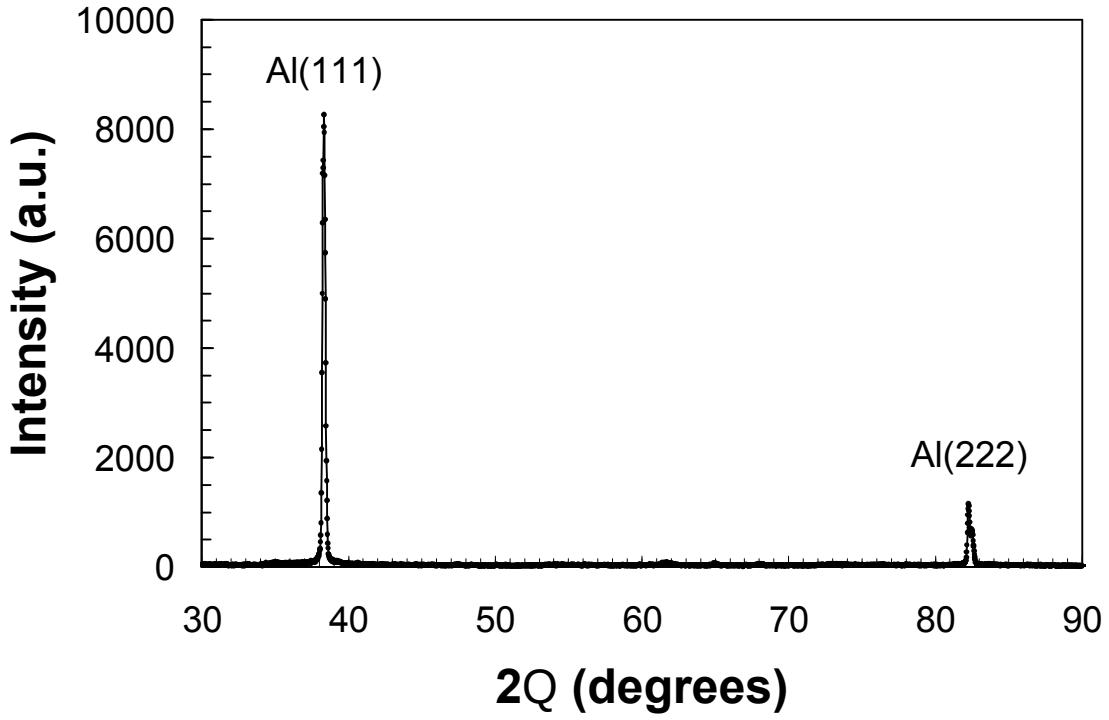
10000
8000
6000
4000
2000
0
Intensity (a.u.)
Al(111)
Al(222)
30
40
50
60
70
80
90
2Q (degrees)

Figure 4.

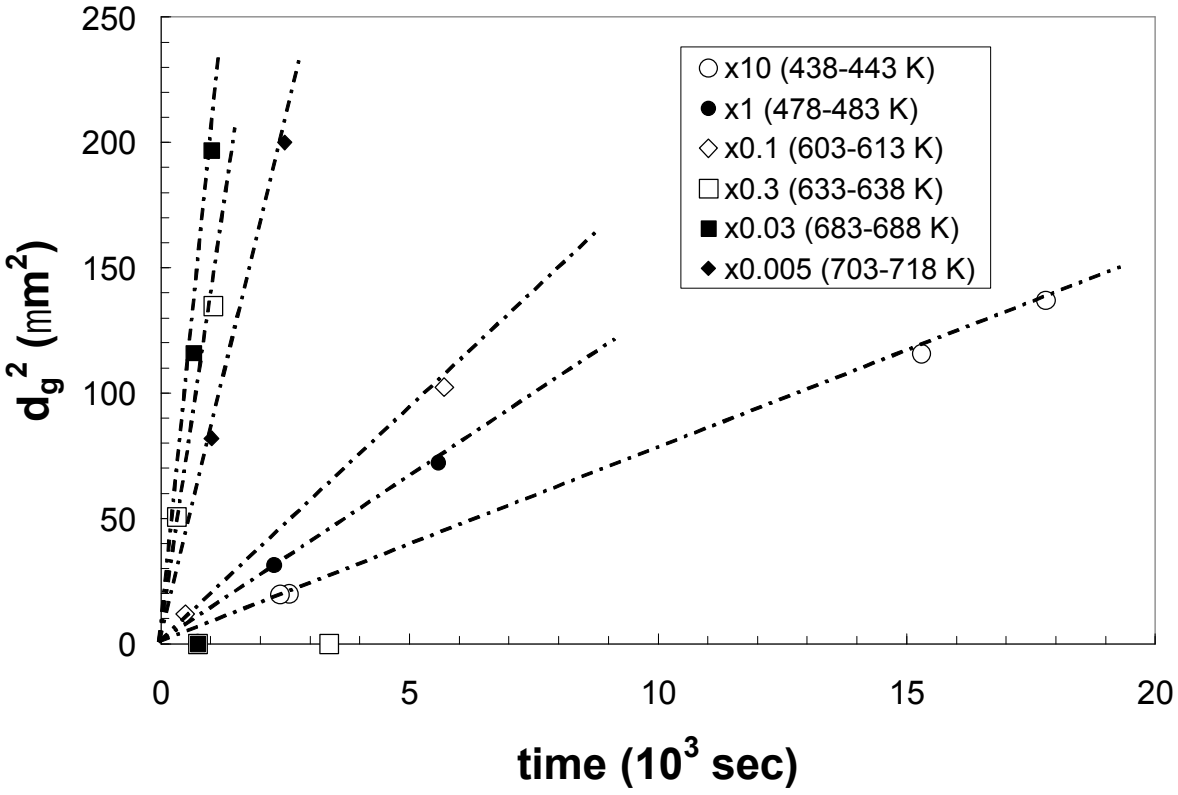
250
200
150
100
50
0
0
5
10
15
20
d_g^2 (mm^2)
time (10^3 sec)
x10 (438-443 K)
x1 (478-483 K)
x0.1 (603-613 K)
x0.3 (633-638 K)
x0.03 (683-688 K)
x0.005 (703-718 K)

Figure 5.

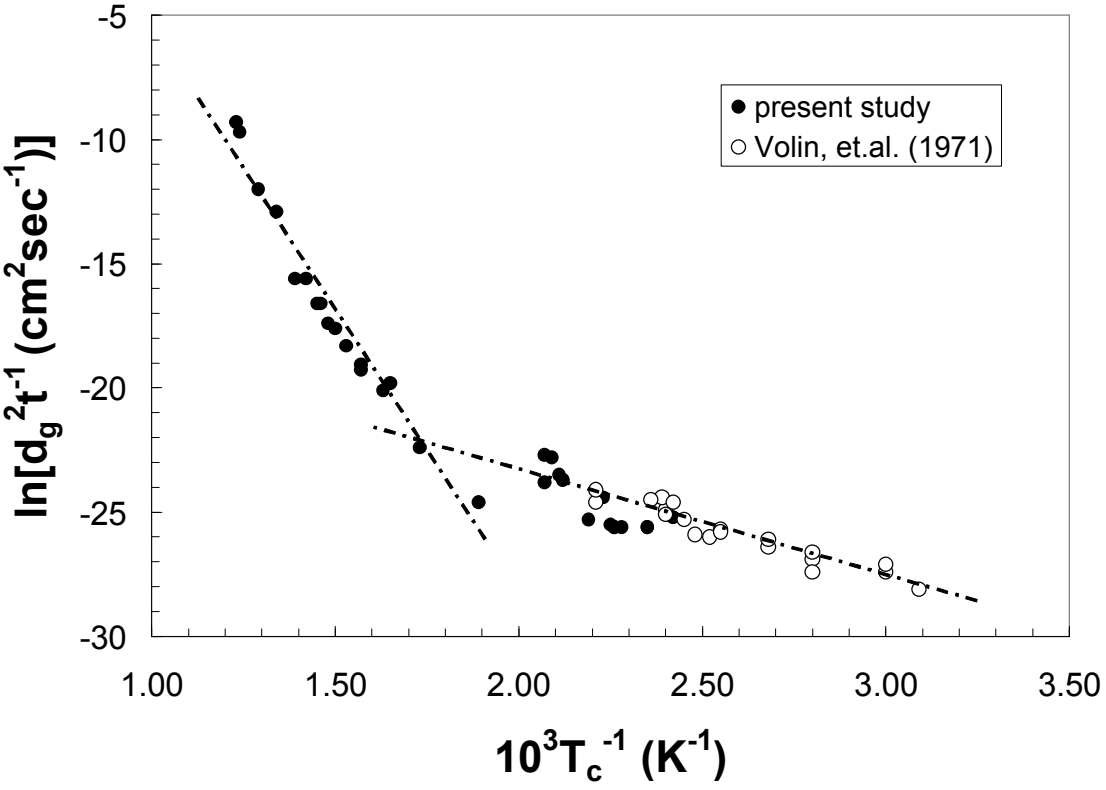
present study
Volin, et.al. (1971)
-5
-10
-15
-20
-25
-30
1.00
1.50
2.00
2.50
3.00
3.50
ln[d_g^2 t^-1 (cm^2 sec^-1)]
10^3 T_c^-1 (K^-1)

Figure 6.